

Potts–percolation–Gauss model of a solid

This article has been downloaded from IOPscience. Please scroll down to see the full text article.

2008 J. Phys.: Condens. Matter 20 075222

(<http://iopscience.iop.org/0953-8984/20/7/075222>)

View [the table of contents for this issue](#), or go to the [journal homepage](#) for more

Download details:

IP Address: 129.252.86.83

The article was downloaded on 29/05/2010 at 10:35

Please note that [terms and conditions apply](#).

Potts–percolation–Gauss model of a solid

Miron Kaufman^{1,3} and H T Diep²

¹ Department of Physics, Cleveland State University, Cleveland, OH 44115, USA

² Laboratoire de Physique Théorique et Modélisation, CNRS-Université de Cergy-Pontoise, UMR 8089, 2, Avenue Adolphe Chauvin, 95302 Cergy-Pontoise Cedex, France

E-mail: m.kaufman@csuohio.edu

Received 13 November 2007, in final form 17 December 2007

Published 31 January 2008

Online at stacks.iop.org/JPhysCM/20/075222

Abstract

We study a statistical mechanics model of a solid. Neighboring atoms are connected by Hookean springs. If the energy is larger than a threshold the spring is more likely to fail, while if the energy is lower than the threshold the spring is more likely to survive. The phase diagram and thermodynamic quantities, such as free energy, numbers of bonds and clusters, and their fluctuations, are determined using renormalization group and Monte Carlo techniques.

(Some figures in this article are in colour only in the electronic version)

1. Introduction

The mechanical properties of solids, such as the mechanical failure, are topics of considerable interest [1–5]. In this paper we analyze an equilibrium statistical mechanics model [6] of a solid. In previous calculations [7] we went beyond the ideal Hooke law for springs by using the realistic anharmonic energy versus atomic distance developed and tested extensively by Ferrante and collaborators [8]. We found that the phase diagram exhibits universal features when the temperature and the stress are appropriately scaled. Those calculations were mean field in character as we assumed that all springs have the same strain. In this paper we evaluate the role of thermal fluctuations by using renormalization group and Monte Carlo simulations. The model is defined in section 2. We view the solid as a collection of harmonic springs. If the energy of such a spring is larger than a threshold, the spring is likely to fail [9]. Assuming that the relaxation times are short compared to the measurement time, we use equilibrium statistical mechanics to compute the various thermodynamic quantities. When the elastic energy is not too large, the partition function for the harmonic ‘springs’ defined on percolation clusters can be mapped into a Potts model [10, 11]. This model is quite similar to the annealed Ising model on percolation cluster [12, 13]. In section 3 we present numerical results based on the renormalization group Migdal–Kadanoff scheme which, as first shown by Berker [14], provides exact solutions of statistical models on hierarchical lattices [15–17] and on small world nets [18, 19]. Monte Carlo simulations are presented in section 4. Our concluding remarks are found in section 5.

³ Author to whom any correspondence should be addressed.

2. Model

The energy of a ‘spring’ (i, j) is given by the Hooke law:

$$H_{ij} = -E_C + \frac{k}{2}(r_i - r_j)^2 \quad (1)$$

where r_i is the displacement vector from the equilibrium position of atom i , measured in units of the lattice constant a , E_C is the cohesive energy, and k is elastic constant. If the energy of the spring is larger than the threshold energy E_0 the ‘spring’ is more likely to fail than to survive. p is the probability that the ‘spring’ survives and $1 - p$ the probability that the ‘spring’ breaks. We assume its dependence on energy to be given by the Boltzmann weight

$$\frac{p}{1-p} = e^{-\frac{K-E_0}{k_B T}} = w e^{-\frac{K}{2}(r_i - r_j)^2} \quad (2)$$

where: $K = k/k_B T$ and $w = e^{\frac{E_C + E_0}{k_B T}}$. We allow for correlations between failing events by using the Potts [10] number of states q , which plays the role of a fugacity controlling the number of clusters [20, 21]: if $q \gg 1$ there is a tendency of forming many small clusters while if $q \ll 1$ there is a tendency to form a few large clusters. If $q = 1$ springs fail independently of one another, i.e. random percolation problem [22]. The partition function is obtained by summing over all possible configurations of bonds arranged on the lattice

$$Z = \sum_{\text{config}} q^C w^B Z_{\text{elastic}}^{\text{config}} \quad (3)$$

C is the number of clusters, including single site clusters, and B is number of ‘live’ (i.e. surviving) ‘springs’. The restricted

partition function associated with the elastic energy for a given configuration of bonds (live ‘springs’) is

$$Z_{\text{elastic}}^{\text{config}} = \text{Tr}_r e^{-\frac{H_{\text{elastic}}}{k_B T}} \quad (4)$$

$$-\frac{H_{\text{elastic}}}{k_B T} = \sum_{(i,j)} \frac{K}{2} (r_i - r_j)^2. \quad (5)$$

In equation (5) the sum is over all live ‘springs’. By using the Kasteleyn–Fortuin expansion [22] for Potts model we can rewrite the partition function as

$$Z = \text{Tr}_\sigma \text{Tr}_r e^{-\frac{\mathcal{H}}{k_B T}}. \quad (6)$$

The Hamiltonian is

$$-\frac{\mathcal{H}}{k_B T} = \sum_{(i,j)} \left[J_1 \delta(\sigma_i, \sigma_j) - \frac{J_2}{2} \delta(\sigma_i, \sigma_j) (r_i - r_j)^2 \right] \quad (7)$$

where σ_i is a Potts spin taking q values. This mapping is a Gaussian approximation valid when, on the right-hand side of equation (7), the elastic energy is small compared to the first energy contribution. The coupling constants J_1 and J_2 are related to the original parameters, w and K , as follows:

$$J_1 = \ln(1 + w) \quad (8)$$

$$J_2 = K \frac{w}{w + 1}. \quad (9)$$

The free energy per bond is: $f = \ln Z / N_{\text{bonds}}$. The derivatives of the free energy f with respect to the parameters w , K , and q provide respectively the number of live ‘springs’ b , the elastic energy E_{elastic} and the number of clusters c , each normalized by the total number of lattice bonds:

$$E_{\text{elastic}} = -K \frac{\partial f}{\partial K} \quad (10)$$

$$b = w \frac{\partial f}{\partial w} \quad (11)$$

$$c = q \frac{\partial f}{\partial q}. \quad (12)$$

The derivatives of those densities, E_{elastic} , b , and c , with respect to the model parameters provide in turn the fluctuations (variances) of those quantities:

$$\Delta E_{\text{elastic}}^2 = -K \frac{\partial E_{\text{elastic}}}{\partial K} + E_{\text{elastic}} \quad (13)$$

$$\Delta b^2 = w \frac{\partial b}{\partial w} \quad (14)$$

$$\Delta c^2 = q \frac{\partial c}{\partial q}. \quad (15)$$

3. Renormalization group

The Migdal–Kadanoff recursion equations [23, 24] for d dimensions are: $Z'_{i,j} = (\text{Tr}_k Z_{i,k} Z_{k,j})^L$, where $L = 2^{d-1}$. We assume each atom coordinate varies in the interval $(-1/2, 1/2)$, where the equilibrium lattice constant is 1. After also using the Gaussian approximation (small elastic energy) we get:

$$w' = [1 + U(w, K, q)]^L - 1 \quad (16)$$

$$K' w' = K \frac{L}{2} [1 + U(w, K, q)]^{L-1} U(w, K, q) \quad (17)$$

where $L = 2^{d-1}$ and

$$U(w, K, q) = \frac{w^2 \text{erf}(\sqrt{K/4})}{q \sqrt{K/\pi} + \sqrt{8} w \text{erf}(\sqrt{K/8})}. \quad (18)$$

The recursion equations (16) and (17) represent the Gaussian approximation of the exact solutions for hierarchical lattices. Since this scheme is realizable, the convexity of the free energy is preserved [25], and thus reasonable expectations, such as positivity of energy fluctuations, are fulfilled. The renormalization group flows are governed by the following fixed points at $K = 0$ (pure Potts model): (i) $w = 0$ (non-percolating live ‘springs’), (ii) $w = \infty$ (percolating network of live ‘springs’), (iii) $w = w_c$ (Potts critical point). A stability analysis at the Potts critical point, ($K = 0, w = w_c$) yields the two eigenvalues: (i) the thermal eigenvalue Λ_1 (for the direction along the $K = 0$ axis) is always larger than 1, meaning the $w - w_c$ is a relevant field; ii. The other eigenvalue Λ_2 is associated with the flow along the $w = w_c$ line away from the pure model ($K = 0$). For $d = 2$, $\Lambda_2 < 1$ for all q . This means that there is a line of points in the (w, K) flowing into, and thus is in the same universality class as, the pure Potts critical point ($w_c, 0$). For $d = 3$ on the other hand, $\Lambda_2 < 1$ for $q < 109$, but $\Lambda_2 > 1$ for $q > 109$. There exists another fixed point at (w^*, K^*) which has both eigenvalues larger than unity for $q < 109$, and becomes stable in one direction for $q > 109$. In figure 1 we show, for $d = 3$, the q dependence of the thermal and elastic eigenvalues associated with the two fixed points. Thus in $d = 3$, for large enough q , the elastic constant K becomes a relevant field changing the universality class of the model from the pure Potts criticality to a new one, Potts elastic. However, in view of the Gaussian approximation used to derive the recursion equations, we view this as only an indication of a possible new universality class that warrants further study.

The phase diagram, figure 2, for any given q , in the (w, K) plane shows two phases: (I) solid with a percolating network of live ‘springs’, (II) crumbling solid with mostly ‘failed’ springs. The two phases are separated by a critical line in the universality class of the q -state Potts model (for $d = 2$ for all q , for $d = 3$ for $q < 109$).

Note that when increasing the elastic constant K , one needs a higher w to establish the solid phase. This is due to the fact that increasing the elastic energy increases the probability for the ‘spring’ to fail.

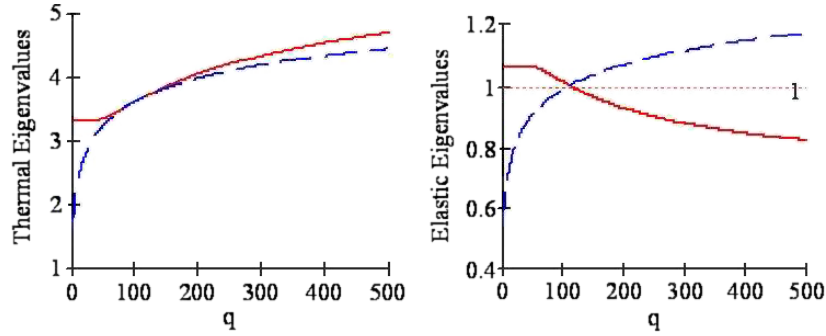


Figure 1. Thermal and elastic eigenvalues in $d = 3$.

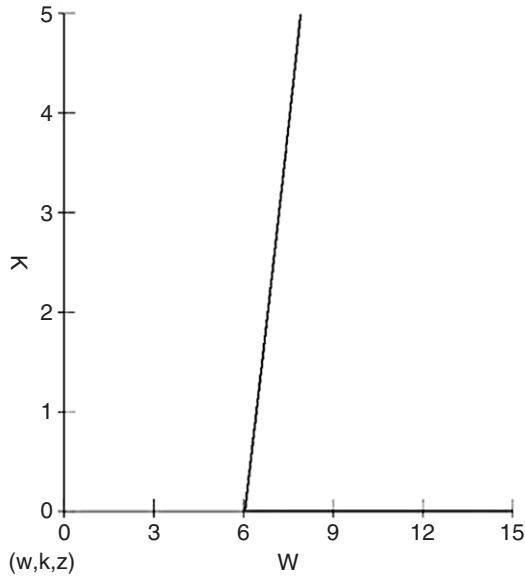


Figure 2. Phase diagram for $q = 10$ and $d = 2$, in the plane (w, K) .

The free energy $f = \ln Z/N_B$, where N_B is the number of lattice edges, is:

$$f = \sum_{n=1}^{\infty} \frac{C_n}{(2L)^n} \quad (19)$$

where

$$C = \ln \left[q + w \sqrt{\frac{8\pi}{K}} \operatorname{erf} \left(\sqrt{\frac{K}{8}} \right) \right]^L \quad (20)$$

and $L = 2^{d-1}$. Using the free energy we can compute the number of live ‘springs’ b , the number of clusters c , the elastic energy E_{elastic} , and their fluctuations (variances). Each of those quantities is scaled by the total number of lattice edges N_B . In figure 3 we show the elastic energy variation with K and w for two different q values. As expected the elastic energy increases monotonically with K and w starting at zero at $K = 0$ and at $w = 0$.

The number of live ‘springs’ increases with w and decreases with K , as shown in figure 4.

We also estimate the squared mean elongation (in units of lattice constant a) of live ‘springs’ by using the number of live

springs, b , and the elastic energy:

$$\Delta r^2 = \frac{2}{K} \frac{E_{\text{elastic}}}{b}. \quad (21)$$

The dependence of Δr^2 on model parameters is shown in figure 5. One can use the classical Lindemann model of melting [26], $\Delta r^2 = 0.01$, to estimate the melting temperature of our model solid.

In the limit $w = 0$, the number of clusters is equal to the number of sites. Hence c approaches the inverse of the coordination number, which for the diamond hierarchical lattice, corresponding to the Migdal–Kadanoff scheme for $d = 2$, is [16]: $c = 2/3$, consistent with figure 6.

In figure 7 we show the elastic energy fluctuations and the number of live ‘springs’ fluctuations as functions of K and w , for $q = 10$ and $q = 1$ respectively. Since the exponent α is positive for $q = 10$ and negative for $q = 1$, a divergence is apparent in the $q = 10$ critical point $K = 2$, $w = 7.3$.

The number of clusters c increases monotonically with the conjugated fugacity q , starting at $c = 0$ at $q = 0$, as shown in figure 8. The fluctuations in c exhibit a divergence at the critical point $q = 10$, $K = 2$, $w = 7.3$ where the critical exponent α is positive.

In figure 9 we show fluctuations in elastic energy, in number of bonds, and number of clusters against w , K , and q respectively, for $d = 3$ and $q = 20$. One can notice the lack of symmetry in the divergence which is a characteristic of $3d$ criticality [27, 28]. By contrast in $2d$ the divergences are symmetric (see figure 7). This is related to the duality transformation [20, 27]. The critical point exponent at $q = 20$, $w = 3.9$, $K = 2$ is $\alpha = 0.015$.

4. Monte Carlo simulations

In this section, we use for Monte Carlo simulation the following Hamiltonian taken from equation (7)

$$\mathcal{H} = -I_1 \sum_{\langle i,j \rangle} \delta(\sigma_i, \sigma_j) + \frac{I_2}{2} \sum_{\langle i,j \rangle} \delta(\sigma_i, \sigma_j) (r_i - r_j)^2 \quad (22)$$

where I_1 and I_2 are renormalized parameters. Of course, one has $J_1 = I_1/k_B T$ and $J_2 = I_2/k_B T$.

In the case of two dimensions $d = 2$, we consider a square lattice of size $N \times N$ where $N = 40, 60, 80, 100$.

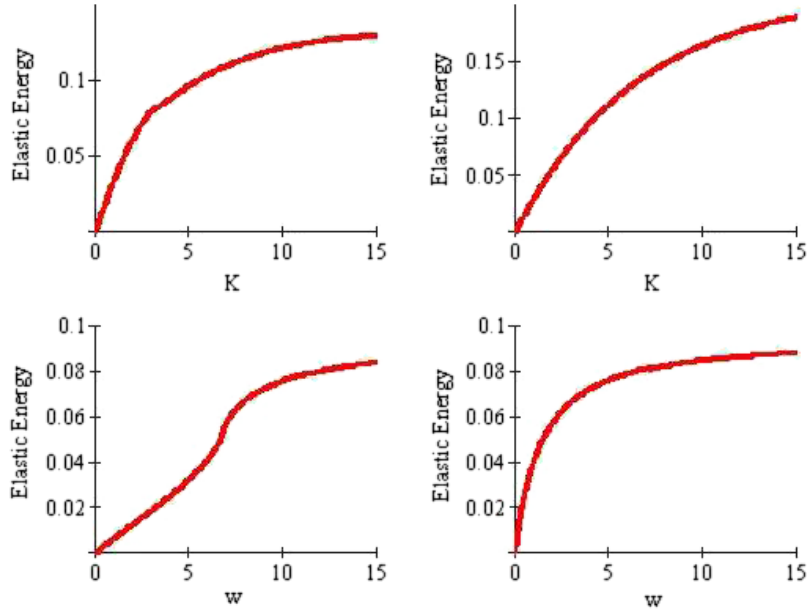


Figure 3. Elastic energy versus K and w . Left column: $q = 10$; right column: $q = 1$.

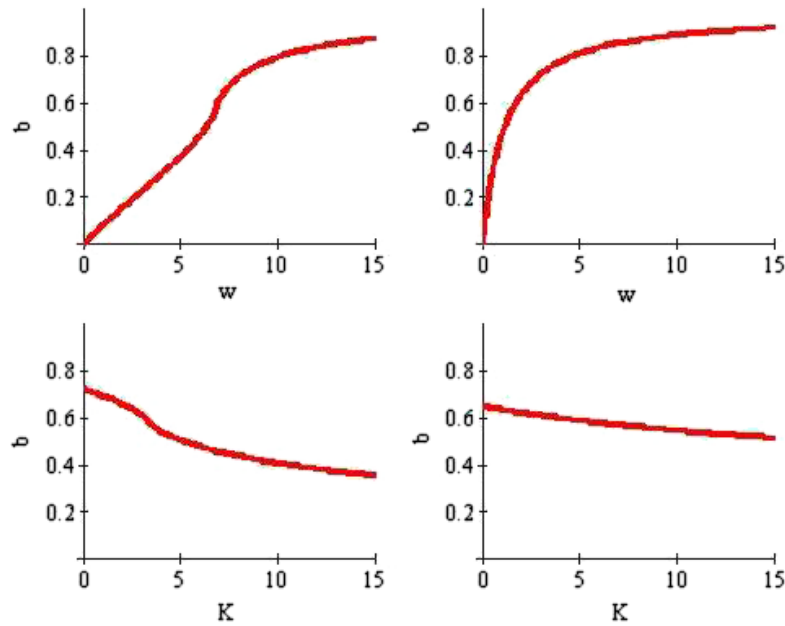


Figure 4. Number of live springs versus w and K , respectively. Left column $q = 10$; right column: $q = 1$.

Each lattice site is occupied by a q -state Potts spin. We use periodic boundary conditions. Our purpose here is to locate the phase transition point and establish the phase diagram. To this end, a simple heat-bath Metropolis algorithm is sufficient [29]. The determination of the order of the phase transition and the calculation of the critical exponents in the second-order phase transition region need more sophisticated Monte Carlo methods such as histogram techniques [30]. These are left for a future study.

The simulation is carried out as follows. For each set of (I_1, I_2) , we equilibrate the system at a given temperature

T during 10^6 Monte Carlo sweeps (MCS) per spin before averaging physical quantities over the next 10^6 MCS. In each sweep, both the spin value and the spin position are updated according to the Metropolis criterion. The calculated physical quantities are the internal energy per spin E , the specific heat C_v per spin, the Potts order parameter Q and the susceptibility per spin χ . For a q -state Potts model, Q is defined as

$$Q = \frac{q \max(Q_1, Q_2, \dots, Q_q) - 1}{q - 1} \quad (23)$$

where $Q_i = \frac{n_i}{N^2}$ ($i = 1, \dots, q$), n_i being the number of sites having q_i .

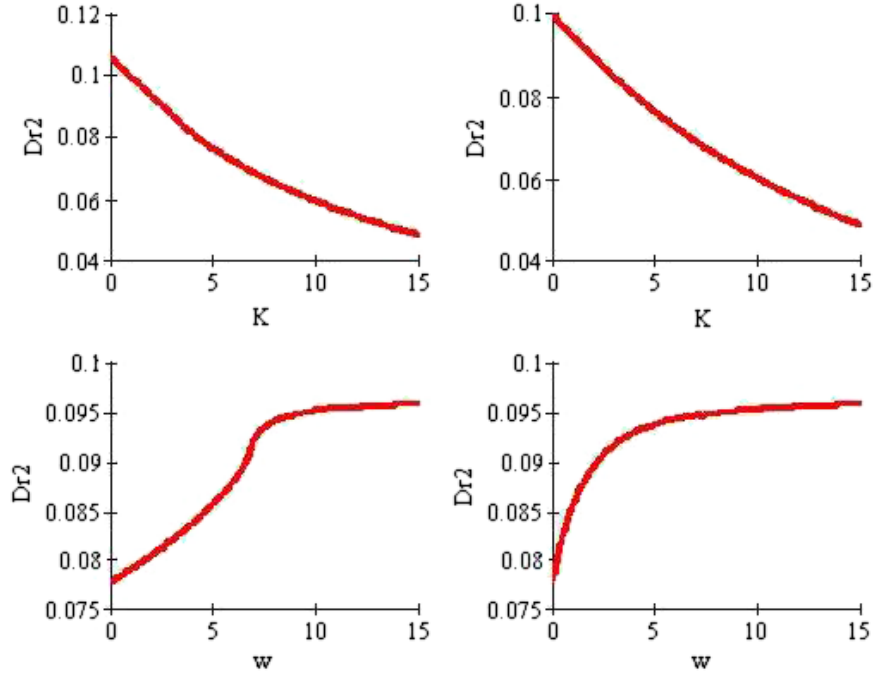


Figure 5. Square of live ‘spring’ elongation versus w and K , respectively. Left column: $q = 10$; right column: $q = 1$.

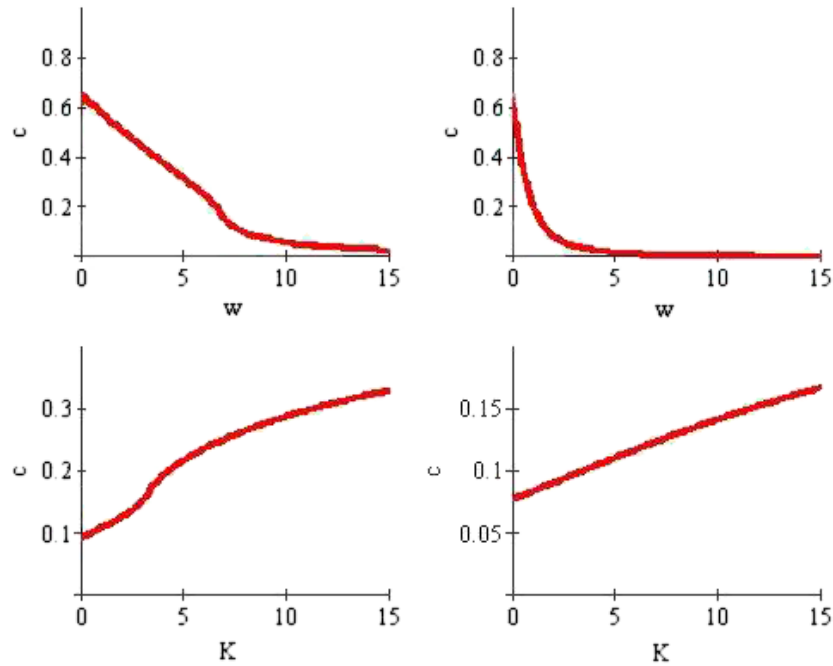


Figure 6. Number of clusters versus w and K , respectively. Left column: $q = 10$; right column: $q = 1$.

Let us show first in figures 10 and 11 the energy, the specific heat, the order parameter and the susceptibility in the case where $q = 2$, $I_1 = 1$ and $I_2 = 0.5$.

These figures show a phase transition at $T_c = 1.130 \pm 0.005$. Note that the size effects for $N = 40, 60, 80$ and 100 are not significant and are included in the error estimation. Simulations have been carried out also for the following sets $(I_1 = 1, I_2 = 0.2)$, $(I_1 = 1, I_2 = 0.8)$ and $(I_1 = 1, I_2 = 1)$.

The results show that the transition temperature T_c does not change significantly with this range of I_2 . T_c depends only on the main I_1 term.

To compare with the results from the renormalization group calculation of the previous section, we have to use $J_1 = I_1/k_B T$, $J_2 = I_2/k_B T$ and equations (8) and (9) to convert J_1 and J_2 into K and w . One has

$$w = \exp(\beta I_1) - 1 \tag{24}$$

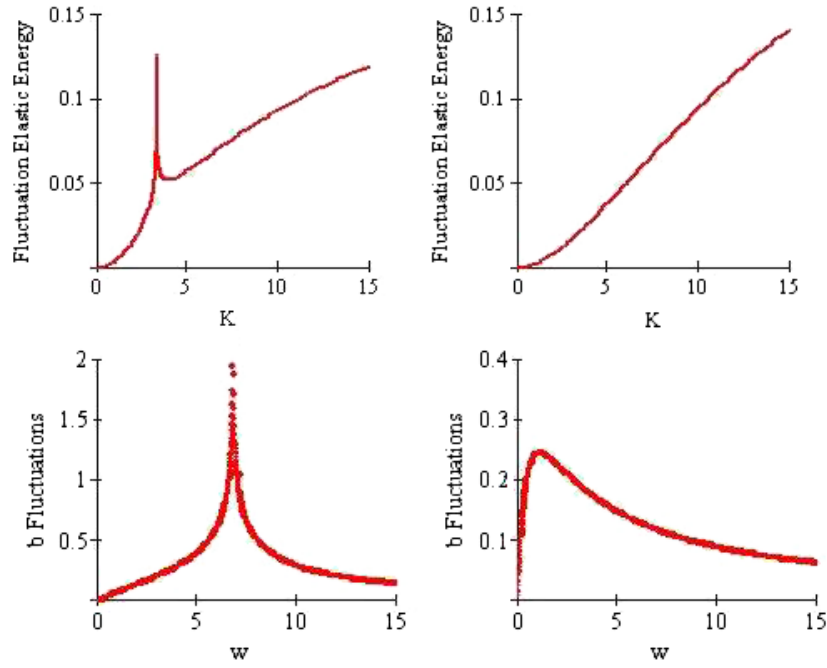


Figure 7. Fluctuations (variances) in elastic energy and number of live ‘springs’ versus K and w , respectively. Left column: $q = 10$; right column: $q = 1$.

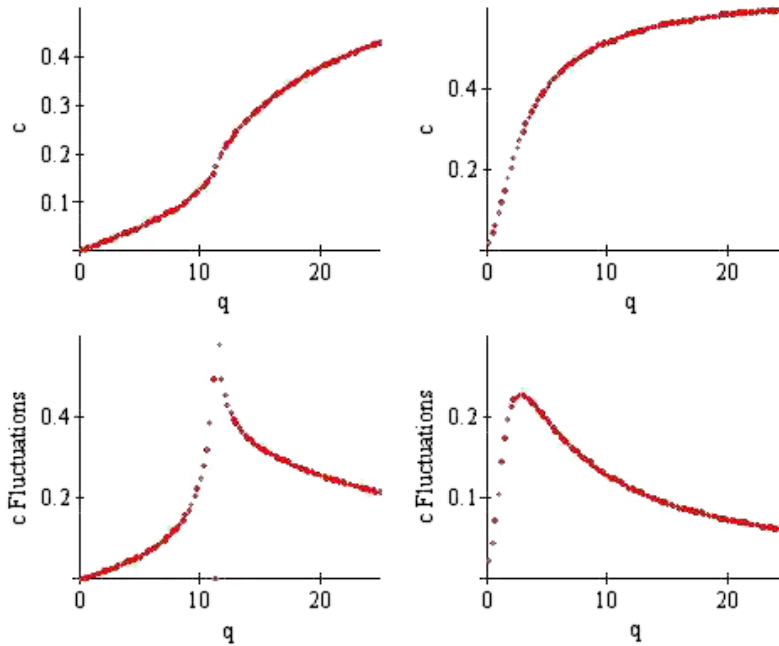


Figure 8. Number of clusters and their fluctuations (variances) versus q . Left column: $w = 7.3$, $K = 2$; right column: $w = 1.857$, $K = 2$.

$$K = \frac{I_2}{k_B T} \frac{1}{1 - \exp(-\beta I_1)} \quad (25)$$

where $\beta = 1/k_B T$.

Figure 12 shows the internal energy E as functions of w and K for $I_1 = 1$ and $I_2 = 0.5$. The transition is found at $w^* = 1.421 \pm 0.002$ and $K^* = 0.753 \pm 0.002$. We observe that only K^* varies with I_2 , not w^* as expected from equations (24) and (25). We have $K^* = 0.301, 1.205$ and 1.506 for $I_2 = 0.2, 0.8$ and 1 , respectively.

5. Conclusions

We have studied a model of a solid made of springs that are live and harmonic or failed. The springs can fail with a probability that increases with the energy. Our renormalization group analysis suggests that elastic perturbations on the Potts–percolation model are irrelevant for all q in two dimensions, and for small enough q in three dimensions. The renormalization group predictions must be viewed as only

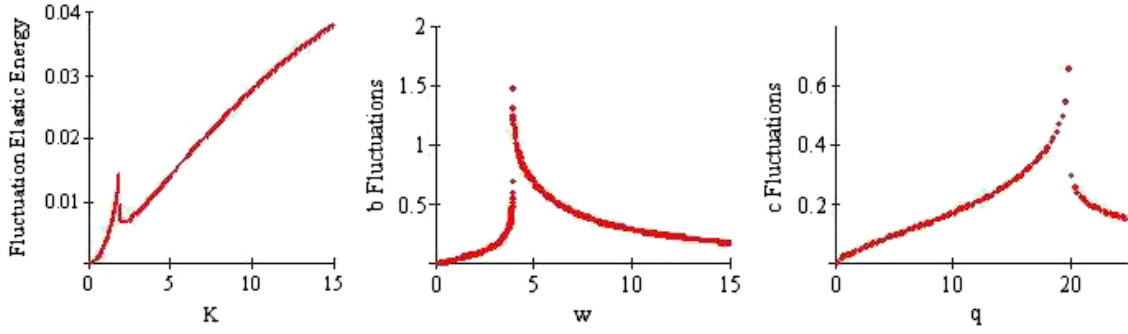


Figure 9. Fluctuations of elastic energy, number of live ‘springs’, and number of clusters versus k , w , and q , respectively, for $d = 3$.

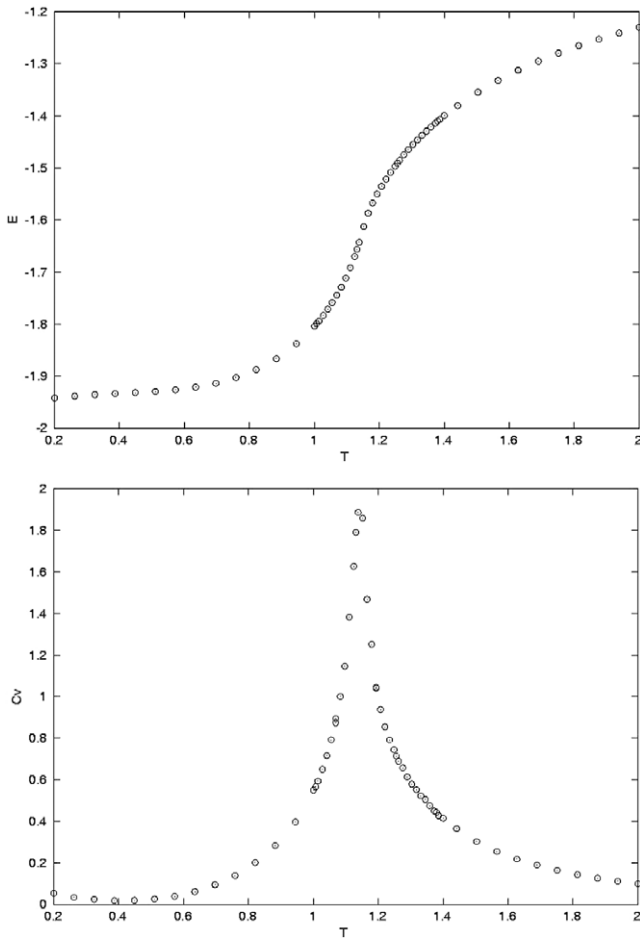


Figure 10. Energy per spin E (upper curve) and specific heat per spin C_v (lower curve) versus temperature T for $q = 2$, $I_2 = 0.5$ with $N = 60$ and $I_1 = 1$.

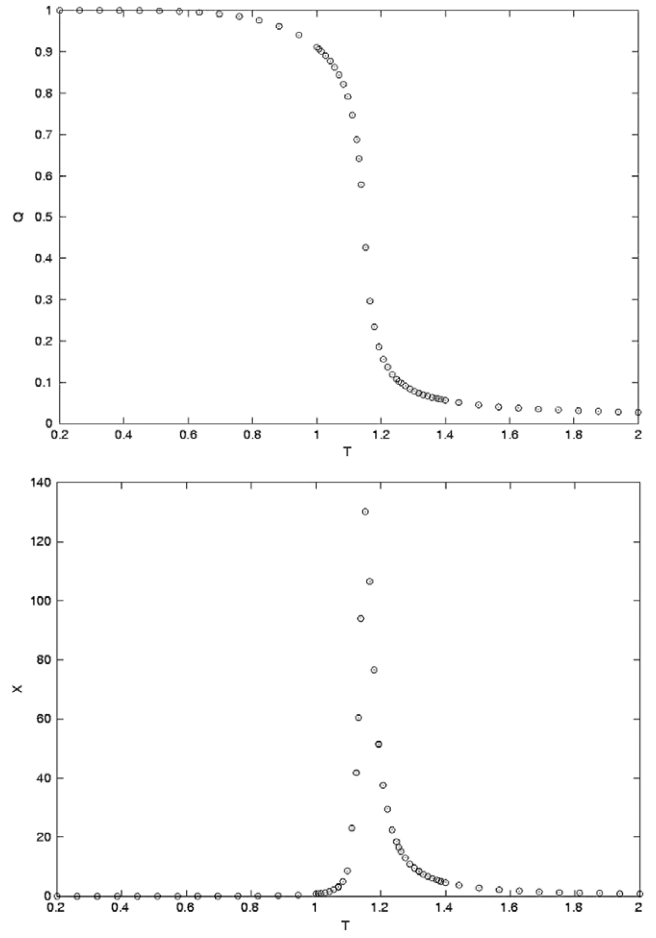


Figure 11. Order parameter Q (upper curve) and susceptibility χ (lower curve) versus temperature T for $q = 2$, $I_2 = 0.5$ with $N = 60$ and $I_1 = 1$.

indicative, in view of the following known limitations. The simple Migdal–Kadanoff renormalization group fails to predict correctly the first-order transitions for $d = 2$, $q > 4$, and for $d = 3$, $q > 2$. Furthermore our recursion equations are valid for small elastic energy. Monte Carlo simulations are needed to further our understanding of the model. Monte Carlo results in $d = 2$ show that the phase transition does not depend on I_2 both on the value of the transition temperature and on the transition order. This is physically in agreement

with the fact that in two dimensions the melting does not take place at finite temperature. At least in $d = 2$, one can say that the phase transition is solely due to the first term of the Hamiltonian (22). We note in passing that in the Ising case, the question of whether the elastic interaction affects or not the Ising universality class has been investigated [31, 32]. No definite conclusions have been reached [33, 34]. It would be therefore interesting in the future to perform Monte Carlo simulations for $d = 3$ and for large q to investigate the

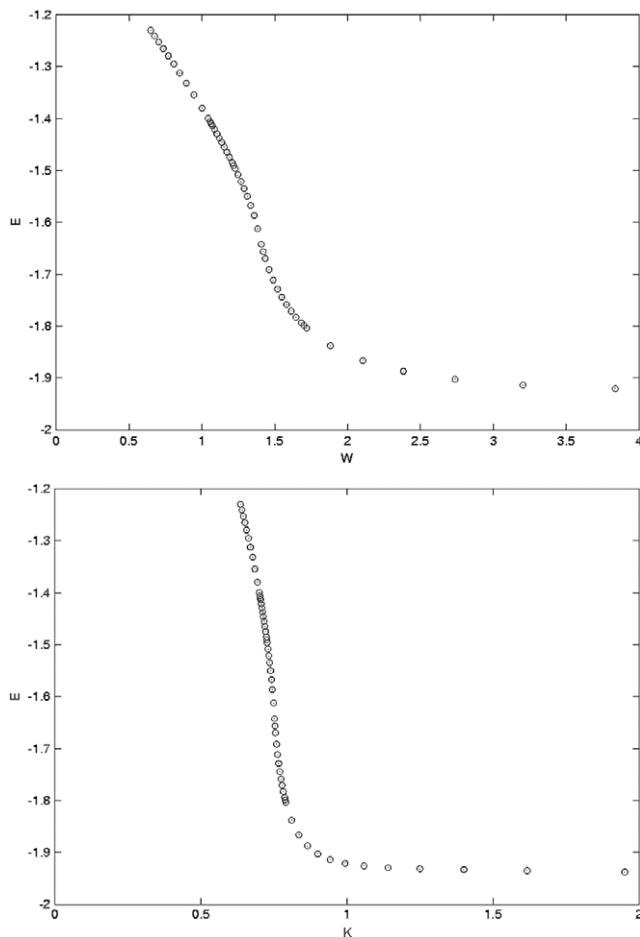


Figure 12. Internal energy E versus w (upper curve) and versus K (lower curve) for $q = 2$, $I_2 = 0.5$ with $N = 60$ and $I_1 = 1$.

effect of elastic interaction on the criticality and on crossover from second to first order. One can expand the percolation–Potts model of a solid to study the equation of state via the Gruneissen approach and fracture by considering ‘springs’ of different elastic constant or threshold energy than the rest of the lattice.

References

[1] De Arcangelis L, Hansen A, Hermann H J and Roux S 1989 *Phys. Rev. B* **40** 877
 [2] Beale P D and Srolovitz D J 1988 *Phys. Rev. B* **37** 5500

[3] Bolander J E and Sukumar N 2005 *Phys. Rev. B* **71** 094106
 [4] Buxton G A, Verberg R, Jasnow D and Balazs A C 2005 *Phys. Rev. E* **71** 056707
 [5] Yanay Y, Goldsmith A, Siman M, Englman R and Jaeger Z 2007 *J. Appl. Phys.* **101** 104911
 [6] Blumberg Selinger R L, Wang Z G, Gelbart W M and Ben-Shaul A 1991 *Phys. Rev. A* **43** 4396
 [7] Kaufman M and Ferrante J 1996 *NASA Tech. Memo.* 107112
 [8] Rose J H, Ferrante J and Smith J R 1981 *Phys. Rev. Lett.* **47** 675
 Rose J H, Smith J R, Guinea F and Ferrante J 1984 *Phys. Rev. B* **29** 2963
 Ferrante J and Smith J R 1985 *Phys. Rev. B* **31** 3427
 [9] Hassold G N and Srolovitz D J 1989 *Phys. Rev. B* **39** 9273
 [10] Potts R B 1952 *Proc. Camb. Phil. Soc.* **48** 106
 [11] Wu F Y 1982 *Rev. Mod. Phys.* **54** 235–68
 [12] Kaufman M and Touma J E 1994 *Phys. Rev. B* **49** 9583
 [13] Scholten P D and Kaufman M 1997 *Phys. Rev. B* **56** 59
 [14] Berker A N and Ostlund S 1979 *J. Phys. C: Solid State Phys.* **12** 4961–75
 [15] Kaufman M and Griffiths R B 1981 *Phys. Rev. B* **24** 496
 [16] Kaufman M and Griffiths R B 1984 *Phys. Rev. B* **30** 244
 [17] Erbas A, Tuncer A, Yucesoy B and Berker A N 2005 *Phys. Rev. E* **72** 026129
 [18] Hinczewski M and Berker A N 2006 *Phys. Rev. E* **73** 066126
 [19] Rozenfeld H D and ben-Avraham D 2007 *Phys. Rev. E* **75** 061102
 [20] Kaufman M and Andelman D 1984 *Phys. Rev. B* **29** 4010–6
 [21] Hu C-K and Chen C N 1988 *Phys. Rev. B* **38** 2765
 [22] Fortuin C M and Kasteleyn P W 1969 *J. Phys. Soc. Japan* **26** (Suppl.) 11
 [23] Migdal A A 1976 *Sov. Phys.—JETP* **42** 743
 [24] Kadanoff L P 1976 *Ann. Phys.* **100** 359
 [25] Kaufman M and Griffiths R B 1983 *Phys. Rev. B* **28** 3864
 [26] Lindemann F A 1910 *Z. Phys.* **11** 609
 [27] Kaufman M 1984 *Phys. Rev. B* **30** 413
 [28] Chase S I and Kaufman M 1986 *Phys. Rev. B* **33** 239–44
 [29] Binder K and Heermann D W 2002 *Monte Carlo Simulation in Statistical Physics* (Berlin: Springer)
 [30] Ferrenberg A M and Swendsen R H 1988 *Phys. Rev. Lett.* **61** 2635
 Ferrenberg A M and Swendsen R H 1991 *Phys. Rev. B* **44** 5081
 [31] Bergmann D J and Halperin B I 1976 *Phys. Rev. B* **13** 2145 and references therein
 [32] Fisher M E 1968 *Phys. Rev.* **176** 257
 [33] Boubcheur E H and Diep H T 1999 *J. Appl. Phys.* **85** 6085
 Boubcheur E H, Massimino P and Diep H T 2001 *J. Magn. Mater.* **223** 163–8 and references therein
 [34] Zhu X, D P Landau and Branco N S 2006 *Phys. Rev. B* **73** 064115